Effects of substrate on the dielectric and tunable properties of epitaxial $SrTiO_3$ thin films

J. H. Hao[a)]
Department of Applied Physics, The Hong Kong Polytechnic University, Hong Kong, People's Republic of China

Zhi Luo and J. Gao
Department of Physics, The University of Hong Kong, Pokfulam Road, Hong Kong, People's Republic of China

(Received 9 May 2006; accepted 10 September 2006; published online 7 December 2006)

Tunable dielectric thin films of $SrTiO_3$ (STO) were prepared on different single-crystalline substrates, including insulating $LaAlO_3$, conductive Nb-doped STO (NSTO), and superconducting $YBa_2Cu_3O_{7-\delta}$. Substrate effects including morphology, orientation, and lattice mismatch induced strains were investigated. We found that a change of substrate used for STO thin films can strongly affect the dielectric properties of STO thin films in terms of dielectric constant, loss tangent, and tunability. Effects of substrate properties on the temperature dependence of dielectric constant and loss tangent were investigated. At low temperatures, STO thin films under minimal strain yield high dielectric constant and low loss tangent while the thin films under either tensile or compressive strain exhibit the reduced dielectric constant and high loss. The tunability of about 77% in STO/NSTO system, close to the value found in STO single crystal, was observed at 10 K. Physical origin of observed phenomena was discussed. © *2006 American Institute of Physics*.
[DOI: 10.1063/1.2392746]

I. INTRODUCTION

Tunable (frequency and phase agile) microwave devices can be achieved with both electric and magnetic fields. The former employs the dielectric tunability of dielectric materials such as ferroelectric $(Ba,Sr)TiO_3$ and incipient ferroelectric $SrTiO_3$ (STO). Low dielectric loss tangent ($\tan\delta$) and large tunability, defined as the ratio between the change of dielectric constant (ε) of materials when applying bias and the dielectric constant without bias, are the key materials parameters for such applications.[1] STO single crystal has quite large tunability of about 80% at 10 K as well as very low loss tangent, $\tan\delta$, is in the range of 10^{-4} at low frequency, rising slightly at low temperatures, where $\tan\delta$ is in the 10^{-3} range. However, the properties of thin films of perovskite titanates have not been compared to the bulk values. Although improved dielectric properties of STO thin films have been reported by a few groups,[2–4] the inferior properties of most reported STO thin films limit their practical applications.

Extensive studies have been carried out to investigate on the mechanisms responsible for much poorer properties of STO thin films. A number of factors such as strain, soft-mode hardening, oxygen vacancy, and interfacial effect have been proposed to explain experimental results.[5–8] In a variety of applications, different substrates have been served as the growth of dielectric thin films. For example, $LaAlO_3$ (LAO) seems to be one of good candidates as a substrate used for microwave devices due to its excellent microwave properties in terms of low loss and dielectric constant. On the other hand, high temperature superconducting $YBa_2Cu_3O_{7-\delta}$ (YBCO) microwave devices are expected to enable low power consumption and efficient frequency utilization in mobile communications systems. The frequency tuning can be achieved by integrating STO thin films into these YBCO devices and tuning the dielectric constant of the STO films by an electrical bias.[9,10] Because of chemical and structural compatibilities of YBCO to STO, STO/YBCO heterostructures are very attractive for tunable microwave devices. Consequently, it is desirable to understand the effects of various substrates on the dielectric and tunable properties of STO thin films.

In this paper, we have deposited epitaxial STO thin films on various substrates, including insulating LAO, conductive Nb-doped $SrTiO_3$ (NSTO), and superconducting YBCO substrates. The structural properties of STO thin films grown on different substrates were measured. A change of substrate used for STO thin films was found to strongly affect the dielectric properties of STO, such as dielectric constant, loss tangent, and tunability. The influence of substrate on the dielectric and tunable properties of STO thin films was discussed.

II. EXPERIMENTS

Prior to the growth of STO thin film, the surface morphologies of substrates were examined by Seiko SPI3800N scanning probe microscope (SPM) using dynamic force mode (DFM). The STO thin films were grown by laser molecular beam epitaxy and pulsed laser deposition. In our recent work,[11] we employed the technique to deposit STO thin films on silicon wafer. A KrF excimer laser (wavelength

[a)]Author to whom correspondence should be addressed; left from Department of Physics, The University of Hong Kong, Pokfulam Road, Hong Kong, P.R. China; electronic mail: apjhhao@polyu.eud.hk

248 nm) was focused on a STO single-crystal target. Insulating LAO, conductive NSTO, and superconducting YBCO in the form of single crystal were used as substrates in this work. To form a parallel-plate capacitor structure for dielectric measurement, conductive NSTO and superconducting YBCO also served as bottom electrodes. For insulating LAO substrate, a 350 nm thick $SrRuO_3$ (SRO) was first deposited on LAO to serve as bottom electrode, and then the STO film was deposited on the SRO layer. Finally, a top Ag electrode was thermally evaporated onto the STO thin films. The STO thin films were deposited at substrate temperature of 700–760 °C in an oxygen pressure of 1.4×10^{-1} mbar. The deposited film was cooled to room temperature in an oxygen atmosphere of 600 mbars.

The film thickness was 300–1000 nm from the measurement of a Dektax[3] ST surface profile. The crystalline phase and structure of the STO thin films were analyzed by x-ray diffraction (XRD) analysis on the Siemens D5000 x-ray diffractometer using θ-2θ and ϕ scan. Dielectric properties were measured using an Agilent 4284A Precision *LCR* meter with option adding ±40 V internal dc bias voltages. The bias voltage dependence of the capacitance and dielectric loss ($\tan\delta$) was measured in a closed-cycle cryogenic system, allowing for a continuous temperature sweep within the temperature range from 10 to 300 K. The measurements were performed at 1 kHz with a signal level of 0.2 Vrms.

III. RESULTS AND DISCUSSION

Figure 1 shows the surface morphology of substrates examined by SPM. The roughness of the substrates was analyzed for imaging data as shown in Table I. It indicates that the roughness of the substrates varied with substrates. Table I also listed the lattice mismatch of the substrates and buffer layer to STO. LAO, although strictly speaking is rhombohedral ($\chi=60°6'$) at room temperature, can be regarded as cubic with a nominal lattice parameter of 0.379 nm. SRO is a distorted perovskite with orthorhombic lattice and has a pseudocubic lattice parameter of 0.393 nm. The lattice constant of STO ($a=0.3905$ nm) is larger than that of LAO and YBCO, indicating that the STO films on LAO and YBCO are under compressive strain. On the contrary, the STO film in the heterostructure of STO/SRO/LAO is under tensile strain as the lattice constant of STO is smaller than that of SRO (in the pseudocubic notation). Thus, different surface conditions and strains due to opposite lattice mismatch along the applied electric field in the parallel-plate capacitor are expected to introduce in the STO thin film deposition.

Figure 2 shows the XRD results of STO thin films grown on various substrates. In the θ-2θ scan of the STO film in Figs. 2(a)–2(d), only the (00*l*) peaks of the STO are present along with those of various substrates and SRO buffer layer. It demonstrates that the STO films grow with *c* axis normal to the substrate/buffer layer. Although a tiny stress in STO/NSTO system was seen by others,[12,13] the diffraction peaks of STO thin film and NSTO substrate overlap in Fig. 2(c), indicating that the near homoepitaxial structures under minimal strain were prepared. The in-plane epitaxial alignment of the STO films was investigated using ϕ scans. Figure 2(e) shows the ϕ scan taken from the (310) peak of the STO films grown on LAO substrates. Only four peaks, 90° apart, were observed for STO thin films. This indicates that the STO film is in plane aligned with the substrate. Similar results of in-plane epitaxial alignment of the STO films were observed in STO films grown on other substrates and/or buffer layer.

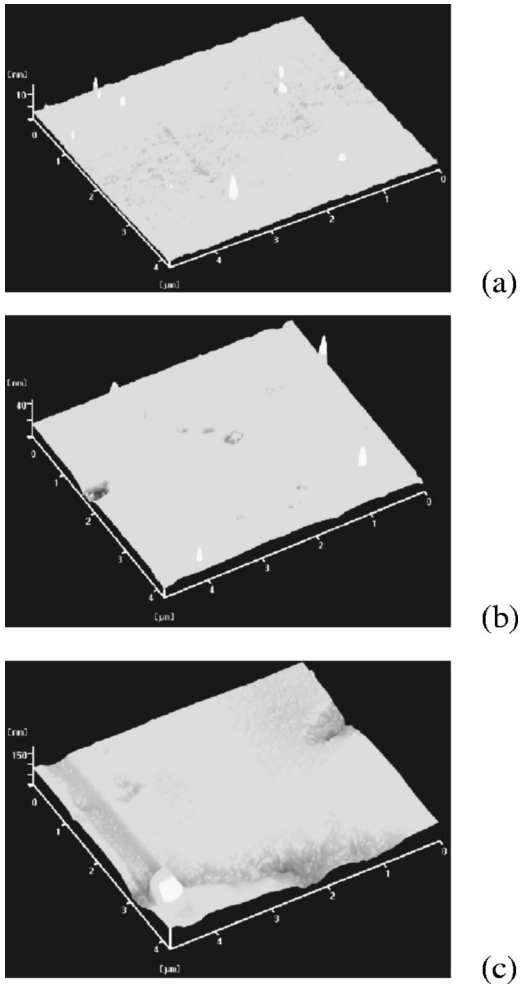

FIG. 1. SPM images of the surface morphology of (a) NSTO, (b) LAO, and (c) YBCO. The roughness of the substrates was analyzed for imaging data.

Low-frequency dielectric constant ε is plotted as a function of measuring temperature for STO thin films on different substrates as shown in Fig. 3(a). To create a parallel-plate capacitor structure, the SRO layer was used as bottom electrode on the insulating LAO substrate. At room temperature, the dielectric constant ε of STO films was about 294, irrespective of the types of substrate. The ε values of films

TABLE I. Roughness of the substrate/buffer layer and lattice mismatch to STO ($a=0.3905$ nm).

Materials	Lattice constant (nm)	Lattice mismatch (%)	roughness (nm)
LAO	$a=0.379$ (pseudocubic)	−2.94	1.038
SRO	$a=0.393$ (pseudocubic)	0.64	···
NSTO	$a\sim0.3905$	~0	0.363
YBCO	$a=0.3823$, $b=0.3887$, $c/3=0.3894$	$a=-2.10$, $b=-0.46$, $c/3=-0.28$	3.638

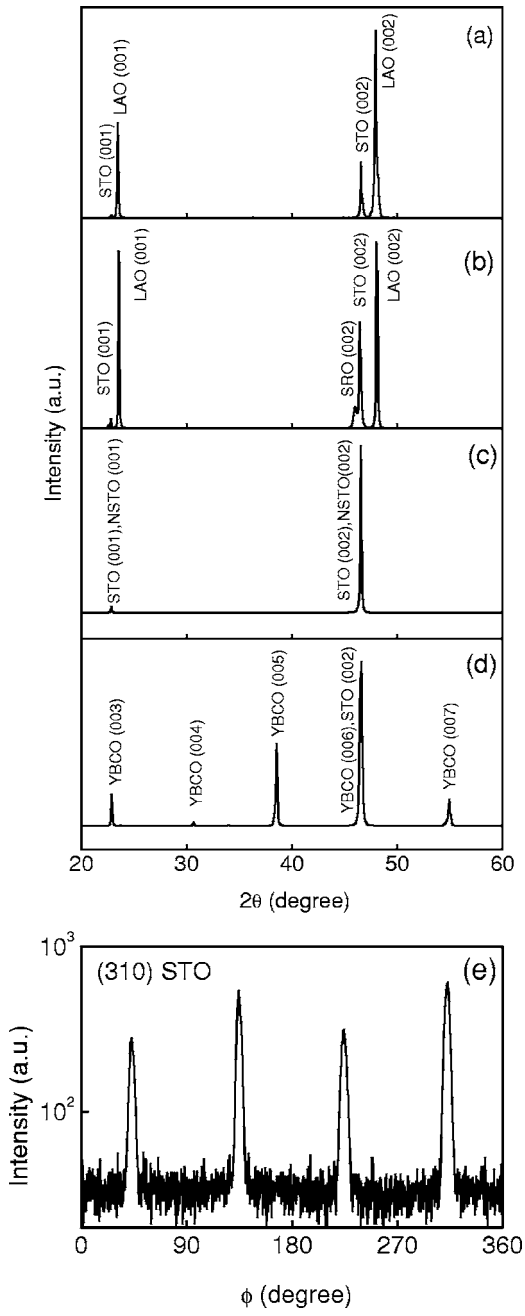

FIG. 2. X-ray diffraction of STO thin films grown on (a) on LAO, (b) SRO/LAO, (c) NSTO, (d) YBCO, and (e) the ϕ scans using the (310) peak for the STO film grown on LAO.

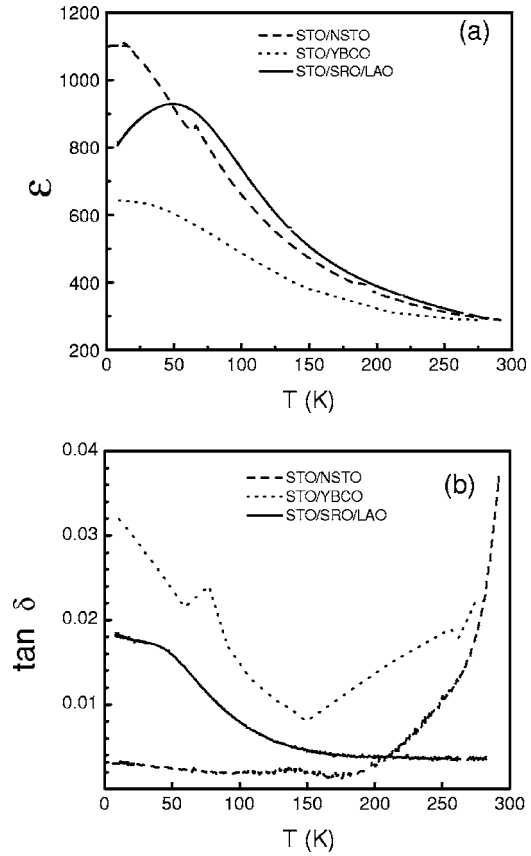

FIG. 3. Temperature dependence of (a) the dielectric constant ε and (b) the loss tangent tan δ of the STO thin films grown on NSTO, YBCO, and SRO/LAO. The measurements were performed at 1 kHz with a signal level of 0.2 Vrms.

grown on all substrates increase as the temperature decreases. However, the ε varies significantly with substrate materials at low temperature. The use of NSTO substrate yields the largest ε of 1115 at 10 K, whereas the use of superconducting YBCO substrate yields the smallest ε of 643 at the same temperature. As most reported STO films, the low-temperature ε here is much lower than the single-crystal value (over 10^4) even in the STO film grown on NSTO. The mechanism responsible for the small dielectric constant in thin films compared to the single-crystal value at low temperature has previously been investigated.[14] The dramatic reduction of the dielectric constant has been attributed to a profound change of the lattice dynamical properties of STO thin films, in particular, of the reduced softening of its lowest optical-phonon mode. In Table I, there are several different kinds of systems, some of them inducing compressive and others tensile stress to STO film. It seems that film's strain, both compression and tension, contributes to the soft-mode hardening in STO thin films. In addition, Lippmaa *et al.* have demonstrated that the step-flow growth mode is critical to acquire very high dielectric constant in STO thin films.[3] It shows that any structural atomic-scale imperfections have a marked influence on the dielectric properties of STO films. The results reported here show the substrate effects on the behaviors of dielectric constant of the films. At low temperatures such as $T=10$ K, STO thin film under minimal strain yields high dielectric constant while the films under either tensile or compressive strain exhibit the reduced dielectric constant. Furthermore, the compressive strain seems to decrease ε more severely as shown in Fig. 3(a). Hyun and Char found that the tensile strain along the applied electric field in the parallel-plate capacitor enhances the dielectric constant and tunability, while the compressive strain decreases them.[6] The results shown in Fig. 3(a) are in reasonable agreement with those reported STO thin films.

Figure 3(b) shows the temperature dependence of the dielectric loss tangent of STO thin films grown on different substrates. The overall loss behavior of those films showed dramatic difference in the choice of substrate within a wide range of temperatures. In STO single crystal, there are two loss peaks that correspond to two phase transitions driven by

the "soft modes," the transverse optical phonons with low frequencies. The high temperature peak at $T=105$ K is associated with the cubic-to-tetragonal (antiferrodistortive) phase transition, which involves the rotation of the Ti–O octahedral. The low temperature peak at $T=10$ K was suggested as an indication of a quantum phase transition into a coherent quantum state. While the high-T peak reflects the elastic properties, the low-T peak is related to the various observed anomalies and is associated with the local Ti–O bond dipoles in STO. A loss peak at about $T=77$ K is observed for the STO film on YBCO in Fig. 3(b), which may be related to the cubic-tetragonal structural phase transition at 105 K for STO single crystal. The temperature dependence of loss tangent of the film on NSTO is quite different from the observation both in STO single-crystal and thin films on other substrates. Above ~190 K, the loss tangent decreases over one order of magnitude as the temperature decreases. Below ~190 K, low loss tangent around 2.0×10^{-3} without significant change was observed within a wide range of temperatures. A lowest loss tan δ is about 1.12×10^{-3} at $T=165$ K. The value is comparable to those best results in previously reported STO films. According to the thickness dependence of dielectric loss in STO films, it is expected that the loss tangent may be close to the loss level found in STO single crystal if the film thickness becomes larger.[2,8] It is known that the intrinsic dielectric loss in an ideal ferroelectric single crystal is related to the multiple-phonon absorption, in particular, those involving the soft-mode phonons. The experimental measurements on STO single crystal can be explained well by the theoretical calculation on the magnitude and temperature dependencies of tan δ. In STO thin films, it is impossible to exclude the existence of defects such as oxygen vacancies, even in high quality epitaxial STO thin films. In STO thin films with defects, one-phonon absorption and phonon scattering on localized phonons near defects may give rise to extra losses. In addition, strain, free carriers, impurity, and interfacial effects are all possible sources of higher loss. Therefore, its is understandable that the STO film under minimal strain (STO/NSTO) exhibits lower loss compared to the STO thin films under either tensile or compressive strains in Fig. 3(b). Furthermore, the effective dielectric behaviors here may depend strongly on the substrate conditions. Low breakdown voltage observed in the STO/YBCO structure reveals the outgrowths of the STO thin films originated from the underlying YBCO substrates. Thus, additional source for the high loss in the STO thin films grown on YBCO may be related to the considerable conduction pathways through the dielectric. Further work on minimizing electrical shorts in STO layer appears to be improving the smoothness of the underlying YBCO.

Tuning measurements were performed on the STO films grown on different substrates. Figure 4 shows the voltage dependence of the dielectric constant of STO thin films grown on (a) NSTO and (b) SRO/LAO at 10 K. Although STO films on YBCO can be tuned with low dc biases of typically 0–4 V, their tuning applied to higher voltage was limited by the high loss mainly due to the aforementioned low breakdown voltage in the STO/YBCO system. During the measurements, the top Ag electrode was kept at a positive bias with respect to the bottom electrode. A decrease in the dielectric constant was observed with increasing electric voltage. The actual tunability of the dielectric constant $[\varepsilon(0)-\varepsilon(V)]/\varepsilon(0)$ of STO films grown on SRO/LAO is 75% over a bias of ±20 V. The observed shift of the maximum of the dielectric constant curves and hysteresis are attributed to the ferroelectric ordering and/or strong charge trapping at the film/substrate interface. On the other hand, the STO film grown on NSTO exhibits 77% dielectric constant tuning at a bias of 20 V, close to the value of 80% found in STO single crystal. Furthermore, the bias dependence of ε is much less symmetrical in the case on NSTO than on SRO/LAO. Generally speaking, an asymmetric property is considered to be due to the work function difference of the top and bottom electrodes in the parallel-plate capacitor geometry. In Fig. 4, it seems not complete if we simply attribute the asymmetric behavior to the work function difference. It is worthy to note that an insulating surface layer forms if NSTO is exposed to oxygen at high temperatures ($T>500$ K) from some researcher's observation.[15] Likewise, the existence of an insulating layer at the interface between NSTO and STO was inferred from dielectric and transport properties of such structures. This is one of possible sources to understand the difference between those two structures.

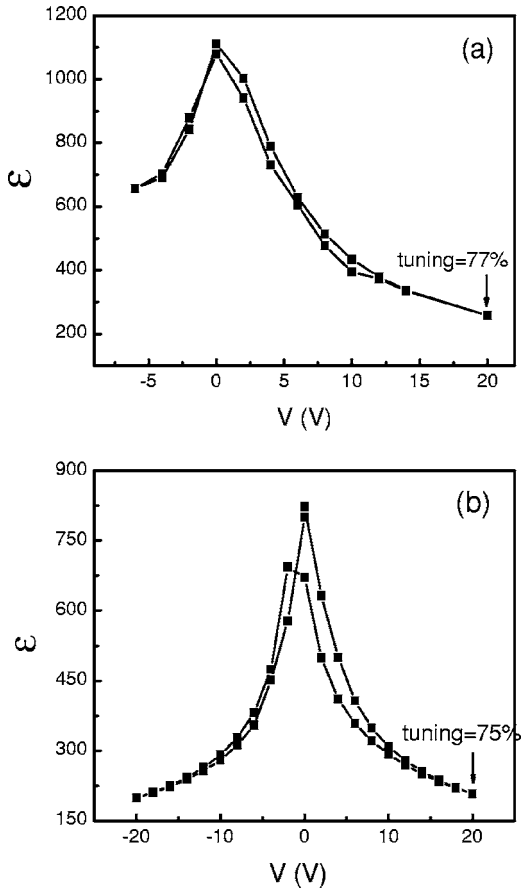

FIG. 4. The electric-bias dependence of the dielectric constant ε for the STO thin films grown on (a) NSTO and (b) SRO/LAO. The measurements were performed at $T=10$ K. The top Ag electrode was kept at a positive bias with respect to the bottom electrode during the measurements.

It is well accepted that the dielectric nonlinearity in STO arises from the hardening of the soft-mode phonon by elec-

tric field. According to the following lattice dynamical theory, [the Lyddane-Sachs-Teller (LST) relation], which connects the frequency of the soft mode to the static ε and optical frequency ε_∞ dielectric constant:

$$\frac{\varepsilon}{\varepsilon_\infty} = \frac{\omega_{\mathrm{LO}}^2}{\omega_{\mathrm{TO}}^2}, \tag{1}$$

where ω_{TO} and ω_{LO} are the zone-center transverse and longitudinal optical mode frequencies, respectively. The dielectric tunability in STO arises from the hardening of the soft-mode phonon by electric field: when an electric field is applied, the soft-mode frequency increases. According to the LST relation, a higher soft-mode frequency leads to a decrease in the static dielectric constant since the frequencies of phonons other than the soft mode do not change much with electric field and temperature.

In STO, the soft-mode behaviors depend strongly on the vibration of Ti and O ions in oxygen octahedral with opposite directions. The STO film grown on NSTO substrate, where the lattice mismatch induced strain is minimal, is expected to be cubic at room temperature. However, the presence of constrains such as strains necessarily lowers the symmetry of the cubic STO system to tetragonal at room temperature. On the basis of the lattice parameter values in Table I, the lattice mismatch between SRO and LAO is 3.69%, while that for the STO/SRO system is only 0.64%. Although the use of buffer layer such as SRO may reduce the strain and interfacial effects, earlier studies indicated that the misfit between the SRO layer and the LAO substrate is mainly accommodated by partial dislocations in the area of the SRO/LAO interface.[16] Some defects propagate through the SRO layer and reach the STO/SRO interface, giving rise to defects in the STO layer from the measurement of high-resolution transmission electron microscopy. Thus, the crystal structure of the STO crystal should be cubic at room temperature; it, in fact, has a little tetragonal distortion in the film layer influenced by the strain due to the lattice misfit between the lattices of STO and substrate and/or buffer layer. The tetragonal phase was observed in films with thickness up to 2.5 μm, suggesting that the lattice mismatch induced strain extends to a large thickness.[8] As a result, the local ordering of the defects and lattice relaxation associated with the defects are related to the substrate conditions. The formation of dislocations at the interface between the STO film and substrate serves to relieve the strain so that the bulk of STO film grows with less stress and fewer defects. The growth mechanism of STO might be different depending on the lattice mismatch with the substrate. The change of any kind of static or dynamic disorder in terms of microstructure and stoichiometry may strongly cause to the difference in dielectric and tunable behavior of STO thin films. Therefore, possible causes for the different dielectric properties of our samples may result from several factors. One is the lattice mismatch listed in Table I. Another possible reason is the obvious change of surface conditions as revealed from Fig. 1 and Table I. It indicates that a difference in interface properties, including film/substrate mismatch and substrate roughness may have contributed to the difference in structural properties. Any structural deviation may give rise to the change in the dielectric properties of titanate perovskites.

IV. CONCLUSIONS

Epitaxial STO thin films and heterostructures have been fabricated on insulating, conductive, and superconducting substrates. We have investigated the effects of a variety of substrates and buffer layers on the dielectric properties of the overlying STO thin films. STO thin films exhibit very different dielectric properties depending on the used substrates. The change of measured dielectric properties of STO films on different substrates are closely related to the different strain and substrate surface. The STO thin films under either tensile or compressive strains exhibit the reduced dielectric constant compared to the near homoepitaxial STO film. Strain and/or rough substrate surface may be associated with the degraded dielectric properties. In the low temperature regime, the values of low loss tangent and high tunability are observed in STO thin films. For example, the tunability of about 77% in STO/NSTO system is close to the value of 80% found in STO single crystal at 10 K.

ACKNOWLEDGMENTS

The authors would like to thank Dr. Z. H. Wang of Nanjing University in providing YBCO single-crystal substrates. This work was supported by grants from the Research Grant Council of Hong Kong (CERG Project Nos. PolyU 7025/04P and PolyU 7025/05P).

[1] J. Hao, W. Si, X. X. Xi, R. Guo, A. S. Bhalla, and L. E. Cross, Appl. Phys. Lett. **76**, 3100 (2000).
[2] H. C. Li, W. Si, A. D. West, and X. X. Xi, Appl. Phys. Lett. **73**, 190 (1998); **73**, 464 (1998).
[3] M. Lippmaa, N. Nakagawa, M. Kawasaki, S. Ohashi, Y. Inaguma, M. Itoh, and H. Koinuma, Appl. Phys. Lett. **74**, 3543 (1999).
[4] H. Takashima, R. Wang, N. Kasai, A. Shoji, and M. Itoh, Appl. Phys. Lett. **83**, 2883 (2003); H. Takashima, R. Wang, M. Okano, A. Shoji, and M. Itoh, Jpn. J. Appl. Phys., Part 2 **43**, L170 (2004).
[5] P. K. Petrov and N. M. Alford, Appl. Phys. Lett. **87**, 222902 (2005).
[6] S. Hyun and K. Char, Appl. Phys. Lett. **79**, 254 (2001).
[7] A. Antons, J. B. Neaton, K. M. Rabe, and D. Vanderbilt, Phys. Rev. B **71**, 024102 (2005).
[8] X. X. Xi, H. C. Li, W. D. Si, A. A. Sirenko, I. A. Akimov, J. R. Fox, A. M. Clark, and J. H. Hao, J. Electroceram. **4**, 393 (2000); A. M. Clark, J. H. Hao, W. D. Si, and X. X. Xi, Integr. Ferroelectr. **29**, A53 (2000).
[9] B. H. Moeckly, L. S. J. Peng, and G. M. Fischer, IEEE Trans. Appl. Supercond. **13**, 712 (2003).
[10] G. Subramanyam, F. W. V. Keuls, F. A. Miranda, R. R. Romanofsky, and J. D. Warner, Mater. Chem. Phys. **79**, 147 (2003).
[11] J. H. Hao, J. Gao, Z. Wang, and D. P. Yu, Appl. Phys. Lett. **87**, 131908 (2005); J. H. Hao, J. Gao, and H. K. Wong, Appl. Phys. A: Mater. Sci. Process. **81**, 1233 (2005).
[12] W. Ramadan, S. B. Ogale, S. Dhar, S. X. Zhang, D. C. Kundaliya, I. Satoh, and T. Venkatesan, Appl. Phys. Lett. **88**, 142903 (2006).
[13] A. Leitner, C. T. Rogers, J. C. Price, D. A. Rudman, and D. R. Herman, Appl. Phys. Lett. **72**, 3065 (1998).
[14] A. A. Sirenko, C. Bernhard, A. Golnik, A. M. Clark, J. Hao, W. Si, and X. X. Xi, Nature (London) **404**, 373 (2000); A. Akimov, A. A. Sirenko, A. M. Clark, J. H. Hao, and X. X. Xi, Phys. Rev. Lett. **84**, 4625 (2000).
[15] H.-M. Christen, J. Mannhart, E. J. Williams, and Ch. Gerber, Phys. Rev. B **49**, 12095 (1994).
[16] J. S. Wu, C. L. Jia, K. Urban, J. H. Hao, and X. X. Xi, J. Mater. Res. **16**, 3443 (2001).